UNIVERSITY OF CALIFORNIA,
IRVINE

Scalable Manufacture of Nanofibers via Near-Field Electrospinning

THESIS

submitted in partial satisfaction of the requirements
for the degree of

MASTER OF SCIENCE

in Material Science and Engineering

by

Tuo Zhou

Thesis Committee:
Professor Marc Madou Irvine, Chair
Professor James Earthman
Professor Frank Shi

2018

DEDICATION

To

my parents

From whom I have got unconditional support and love,

From whom I know hard-working is more important than talent,

From whom I realized knowledge is more precious than treasure.

TABLE OF CONTENTS

Page

LIST OF FIGURES iv

LIST OF TABLES vii

ACKNOWLEDGMENTS vii

ABSTRACT OF THE THESIS ix

1.INTRODUCTION 1
1.1: Brief introduction to nanotechnology and MEMS/NEMS system: 1
1.2: Brief introduction to electrospinning technology 3
1.3. The photolithography 18
1.4. pyrolysis 20

2.Material and Method 21
2.1. Polymeric solutions preparation 21
2.3. Near-field electrospinning setup 23
2.4 Optimization of the process parameters 26
2.5. Fabrication of the supporting structure to nanofibers by photolithography 26
2.6. Suspension test of nanofiber 31

3. Results and Conclusions 32
3.1. Scalability and deposition control 32
3.2. Effects of the process parameter on the size of obtained nanofibers 34
3.3. Effects of the process parameter on the spacing between each obtained nanofibers 40
3.4. Suspension test of fiber 44

4.Furture works 46

5. Bibliography 48

LIST OF FIGURES

Page

Figure 1: Scale of items in nanometers 2

Figure 2: Early electrospinning setup developed by Baumgartn[6]. 5

Figure 3: Number of electrospinning-related patents and publication (red) and citation (blue) per year since 2001[4]. 6

Figure 4: The schematic illustration of horizontal electrospinning setup.[19]. 7

Figure 5: The electrospinning with vertical(left) and customized angular feeding(right) direction 7

Figure 6: The schematic early processes of the fiber initiation. (A) under the influence the electrical field, some charges accumulate on the surface the polymer droplet. (B) Deformed droplet attributed to the repulsion force generated by each charge. (C) Further deformation of the droplet and transferred into the form of Taylor cone and fiber initiation at the tip of it [2]. 8

Figure 7： The evolution of a droplet from spherical-like shape into the conical-like Taylor cone 9

Figure 8:The illustration of the fiber emanated from the droplet 9

Figure 9: Illustration of the path of the fiber jet during electrospinning process 10

Figure 10: Schematic of a conventional vertical feeding electrospinning setup 15

Figure 11: The image of in-house far-field electrospinning setup 16

Figure 12: The image of the deposited 10% PAN obtained by the in-house far-field electrospinning 16

Figure 13: Image of the in-house electromechanical spinning 17

Figure 14: The schematic of EMS process 18

Figure 15: Steps of photolithography process 19

Figure 16: Picture of PAN and its solvent DMF 21

Figure 17: The PAN-based solutions 22

Figure 18: The syringe filled with 9% of PAN 22

Figure 19: The in-house novel near-field electrospinning setup 24

Figure 20: The zoomed-in picture of the crucial syringe setting 24

Figure 21: Picture of syringe pump controller 25

Figure 22: Moving stage controller (right) and voltage supply (left) 25

Figure 23: Schematic of supporting structure 26

Figure 24: The spin coating for SU-8 2015 28

Figure 25: Soft-bake of coated silicon wafer 29

Figure 26: Temperature Ramp used for soft bake 29

Figure 27: The expose step by using UV radiation 30

Figure 28: Illustration of the fiber collection by the rotating drum 33

Figure 29: The nanofiber obtained by EMS (left) and new setup (right) at same applied voltage 33

Figure 30: Nanofibers obtained by new setup with 500V, 480um/s stage speed 34

Figure 31: The images of fibers obtained 11% of PAN fibers at different voltages 35

Figure 32: The relationship between Voltage and diameter of fibers 36

Figure 33: Images of 11% PAN fiber at different RMP 37

Figure 34: The relationship between diameter of fiber and RPM 37

Figure 35: The images of working distances 38

Figure 36: The images of obtained fibers regarding to each distance 39

Figure 37: The relationship between working distance and diameter of fibers 40

Figure 38: Some selected images of 11% of PAN fibers obtained at various RPM 41

Figure 39: Relationship between RPM and spacing 42

Figure 40: Some selected images of fibers obtained at various stage speed 43

Figure 41: The relationship between stage speed and inter-fiber spacing 44

Figure 42: The suspended or dripped fibers made by 11% PAN 45

Figure 43: The hole at the back of chamber of woven Figure 44: Nanofibers in the form 46

LIST OF TABLES

Page

Table 1: The working distance and diameter of the fibers 40

Table 2:The value of RPM and spacing between fibers 42

Table 3: The stage speed and the resulting spacing between fibers 43

ACKNOWLEDGMENTS

First, I would like to express my most genuine appreciation to my thesis advisors, professor Marc Madou, who offered me this valuable opportunity to work with him and his fabulous student, their advice and guidance on both my research and career through the development of my master thesis work has been invaluable and made this opportunity a life changing experience.

I would also like to thank my parents who has offer a great life-experience in united states, only gold know how much I love them.

I would also like to thank all my lab mates in UCI Bio MEMS lab.

ABSTRACT OF THE THESIS

Scalable Manufacture of Nanofiber via Near-Field Electrospinning
By

Tuo Zhou

Master of Science in Material Science and Engineering

University of California, Irvine, 2018

Professor Marc Madou Irvine, Chair

Carbon nanofiber has been gaining traction due to its broad application. Nanofibers have been successfully produced by various fabrication method, such as extrusion or hot-wire drawing. Shortcomings of these methods, such as low-efficient and, high-cost, preventing it from becoming a scalable manufacture process. Alternatively, electrospinning is a low-cost and high-efficient technique capable of manufacturing larger quantities of fibers in a relatively short period. Even though, the conventional electrospinning method, far-field electrospinning has become commercialized for production of large bundles of nanofiber, it is incapable of producing ordered and orientated fibers. Unfortunately, many need the precise control of the fiber deposition which is difficult with the far-field electrospinning. This limitation was resolved using near-field electrospinning, which could fabricate the fibers in a controllable, economical and rapid way.

Before this research, various near-field electrospinning apparatuses were developed to enhance the controllability of the fiber deposition. For example, our lab (UCI Bio-MEMS Lab)

has developed a new electromechanical spinning (EMS) technology. Compared with the previous electrospinning method, the precise deposition of single suspended fibers has been achieved, but scalability and throughput still need to be improved.

Therefore, we built a novel new electrospinning system inspired by the existing EMS and conventional far-field electrospinning system. The system has successfully produced the aligned nanofibers with a diameter on the magnitude of nanometer and micrometer. More importantly, this new approach could generate hundreds of nanofibers in less than a minute. The process parameters of this new system, including the applied voltage, stage speed of the needle, working distance between the needle and collector and the rotation speed of the drum, on fiber diameter and fiber alignment are reported in this thesis. This new method of near-field electrospinning has outperformed the existing electrospinning techniques as a potential for scalable nanofiber manufacturing.

1.INTRODUCTION

1.1: Brief introduction to nanotechnology and MEMS/NEMS system:

Nanotechnology has gained huge attention in both the industrial setting and research field owing to its novel properties and unpredictable potential on chemical, physical, and biological system at scales ranging from a single atom to submicron dimensions. Previous nanotechnology research has achieved breakthroughs in many fields, which including material science, nano-manufacture, nanoelectronics, healthcare, energy storage, bio-engineering and even national security[1]. Nanotechnology is expected to have an essential and revolutionary influence on society and economy in the future.

Micro-or nanoelectromechanical system (MEMS/NEMS) are the devices combining electrical and mechanical components that have a characteristic length less than 1 mm and 1 μm respectively. Micro- and nanosystem components are commonly fabricated by top-down lithography techniques. Figure 1 provides a better understanding of the scale of items in micro and nanometer range.

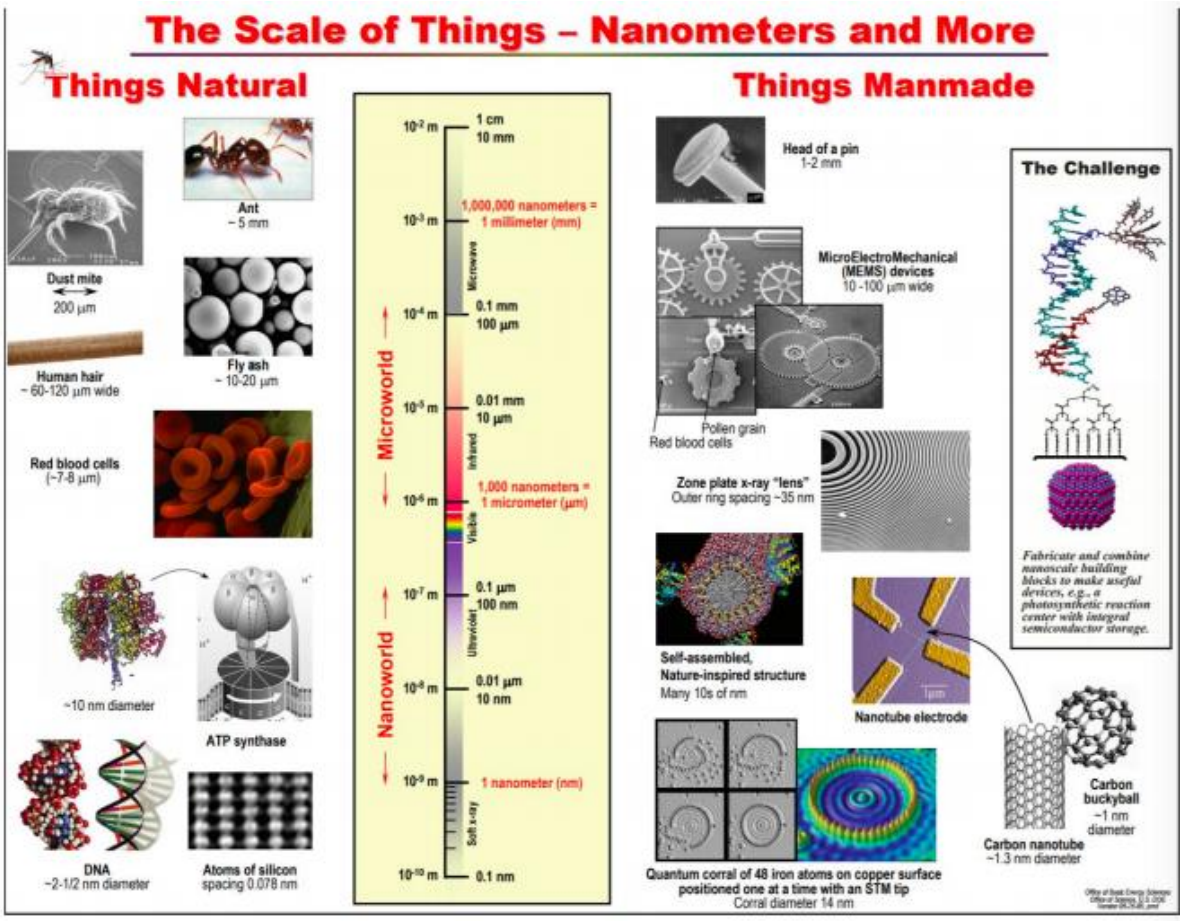

Figure 1: Scale of items in nanometers

MEMS/NEMS device are dominated by silicon-based mature microfabrication technologies. However, many additional promising materials have sought after for the fabrication of the MEMS and NEMS devices, such as metal and polymeric materials[2].

Among those new materials, carbon-based micro- and nanodevices have gained more interest and attention recently due to its versatility and potential for applications in diverse fields. Other benefits of carbon-based devices include a scalable manufacturing process, inexpensive and readily available precursor polymeric materials, tunable surface properties

and biocompatibility. Photolithography followed by carbonization is a robust method to fabricate these carbon-based MEMS. However, other techniques better than lithography have been developed.

Among all kinds of nanostructures, one-dimensional (1D) nanostructures, such as wires, rods, tubes, and fibers, has received lots of attention due to their unique and remarkable applications in nanoscale devices. Therefore, they were expected to play an essential role as interconnects and functional units in the fabrication of electrochemical devices with nanoscale dimensions. Although the 1D nanostructures can be fabricated by carrying out many existing advanced lithographic techniques, such as electron-beam, X-ray, and UV lithography, further developments of scalability, cost-saving are needed[3],[4].

Regarding those challenges, electrospinning techniques was invented as a straightforward and cost-saving method to fabricate 1D nanostructures. In principle, electrospinning technique is to utilize the electrostatic forces to draw the fiber jet from the conductive polymer solution or melt. By adapting conventional electrospinning setups, continuous nanofibers can be fabricated with various diameters in desired configurations[5],[6].

1.2: Brief introduction to electrospinning technology

1.2.1: Background and history of electrospinning

Electrospinning, also termed electrostatic spinning, is a convenient process to manufacture ultra-thin and ultrafine polymer nanofibers with unique physical, chemical, electromagnetic and optical properties through a relatively economically efficient method[7][8], [9].

Electrospinning utilizes electric forces to extrude millimeter to nanometer fibers from conductive polymer solution, or melt.

Compared to other fiber fabrication techniques, such as chemical growth, dip-pen lithography, and thermal extrusion. Despite fancy merits and increasing popularity the electrospinning has gained in this decade, it's actually an undeniable old technology which could be dated back to the early 1890's when it was first discovered by Rayleigh. From 1934 to 1944, Formals [10] had designed and built an experimental setup to specifically produce polymer filaments by applying electrostatic field. In 1952, Vonnegut and his team successfully produced 0.1 mm diameter droplets, which was latered classified as a variation of electrospinning [11]. In 1966, Simons [10]successfully created an apparatus to produce small and light non-woven fabrics. Since 1980, the electrospinning has developed to armature level and regained more interested because of bio-engineering application. The modern general electrospinning process and setup resemble what Baumgarten[12] and his team created in 1971 shown in Figure 2. To date, more than one hundred polymer solutions have been successfully electrospun to obtain ultrafine nanofibers illustrating the versatility and potential of this technique.

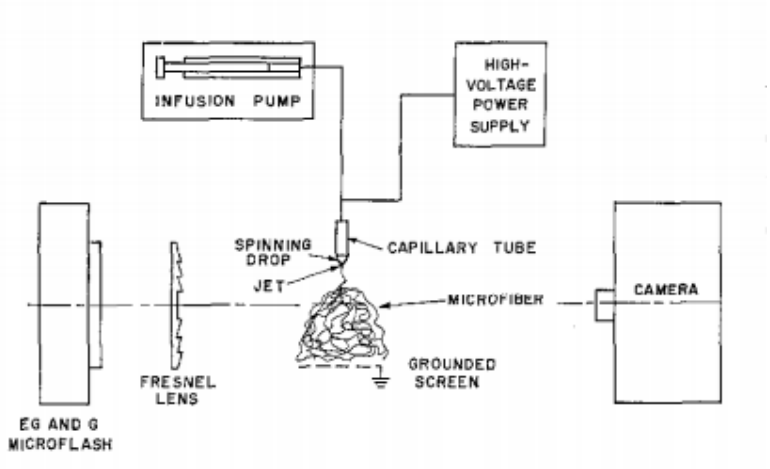

Figure 2: Early electrospinning setup developed by Baumgartn[6].

The number id universities and research intuitions contributing to the field of electrospinning is rapidly growing due to the interdisciplinary applications such as tissue engineering[13], drug delivery[14], filtration[15], sensing [16] and energy storage [17], [18]. Figure 3 illustrates the growing trend of the amount of electrospinning-related publication and patents [4]. Although electrospinning is very convenient and straightforward, the understanding of the physics governing the fiber extrusion behavior is limited. This thesis is focus on the characterization of the manufactured fibers and basic explanation on its mechanism will be provided.

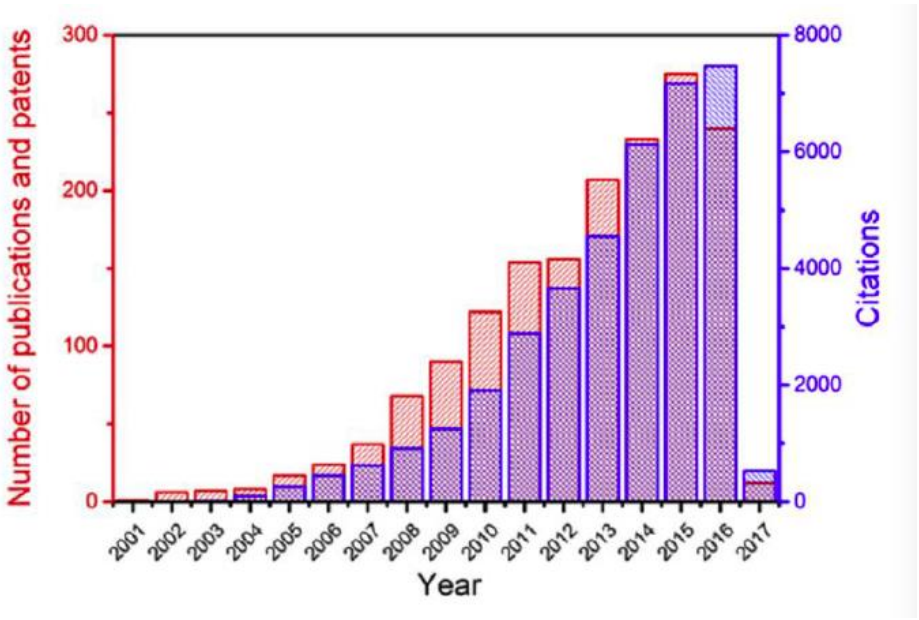

Figure 3: Number of electrospinning-related patents and publication (red) and citation (blue) per year since 2001[4].

1.2.2 Mechanism of electrospinning

Setup

The conventional electrospinning set-up includes four main components:1)a high voltage source which generates the electrostatic force required to form fibers, 2)the polymer solution source continuously supplying the polymer precursor3)the conductive extrusion tip where the high voltage is applied and 4)the grounded collector could collects the electrospun fibers[7], figure 4 is a simplified schematic of a horizontal electrospinning set up, but various configurations are capable of achieving the same fiber seen in figure 4. Depending on the different properties or requirements of the final fibers, some components could be changed or added, such as rotating drum collector typically used to obtain aligned fibers.

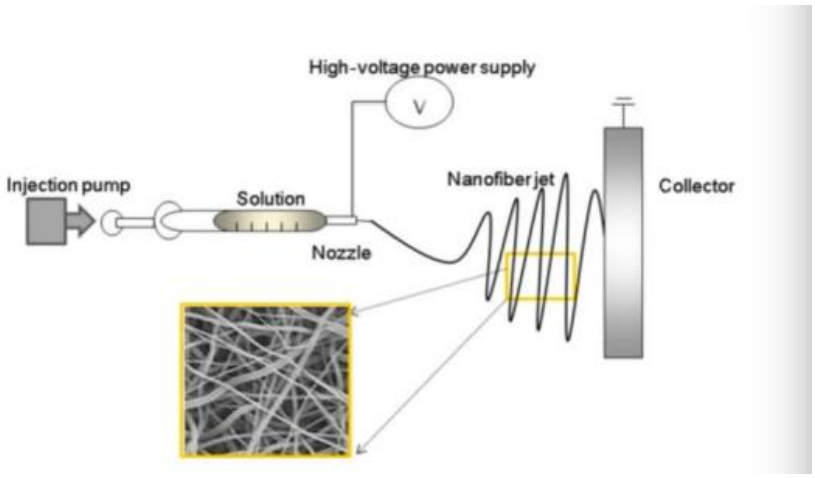

Figure 4: The schematic illustration of horizontal electrospinning setup.[19].

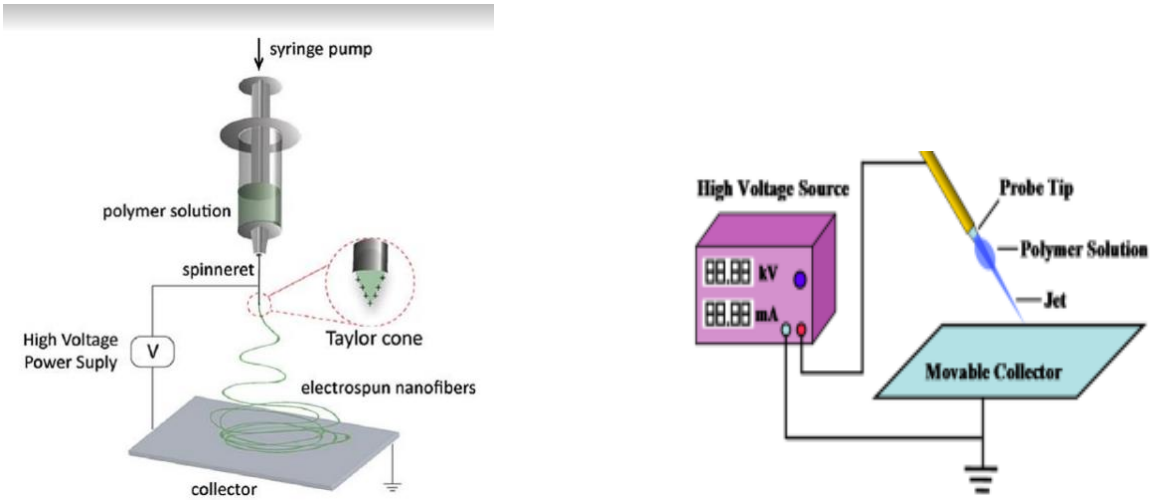

Figure 5: The electrospinning with vertical(left) and customized angular feeding(right) direction

Taylor cone and fiber jet initiation

The electrostatic field plays a big role in the electrospinning process where the large electric field gradient conductive polymer solution was accelerated towards to the direction of where the collector located which carry the opposite charges, once the polymer solution

reached the tip of spinneret, a pendant drop with accumulated induced charged on its surface would be formed there and the surface tension of the droplet would hold it from dripping. And with the gradually increasing electrostatic field, the repelled force generated by the charges would overcome the surface tension eventually and, therefore, lead to the emanation of the fibers from the droplet in the form conical shape, which is termed Taylor cone[8]. Figure 5 briefly demonstrated the first steps of fiber initiation and formation of Taylor cone.

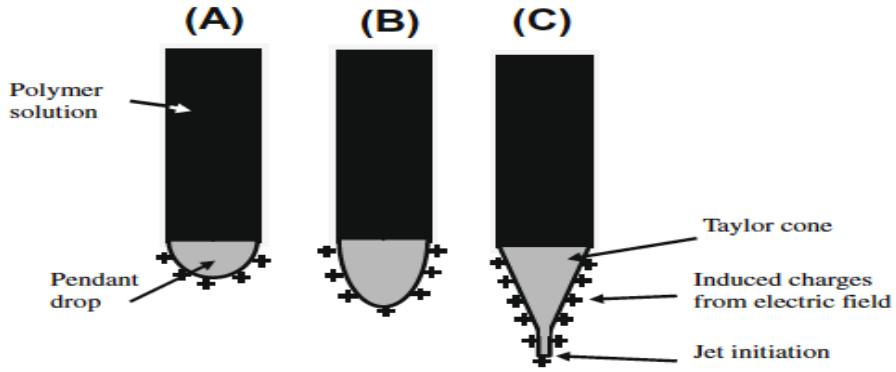

Figure 6: The schematic early processes of the fiber initiation. (A) under the influence the electrical field, some charges accumulate on the surface the polymer droplet. (B) Deformed droplet attributed to the repulsion force generated by each charge. (C) Further deformation of the droplet and transferred into the form of Taylor cone and fiber initiation at the tip of it [2].

Many factors affect the formation and size of the Taylor cone. Nonetheless, the magnitude of the electric field is the most significant force acting on the polymer solution. Once the droplet was form at the tip of the conductive needle, the interaction of the charges distributed on the surface and the external electrical field cause the deformation of the droplet. The droplet under the influence of the electric-field stretches to a conical shape, referred as Taylor cone as mentioned before, with the growing electric field applied between the needle and collector. Figure 7and 8 illustrate the process of a vertical droplet under a growing electric

field. The first image demonstrates the rounded shape as it slowly converts to the conical shape until the jet was formed.

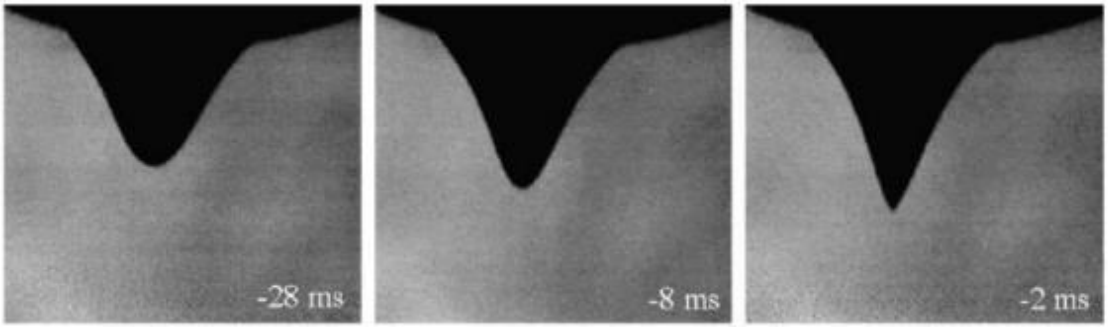

Figure 7： The evolution of a droplet from spherical-like shape into the conical-like Taylor cone

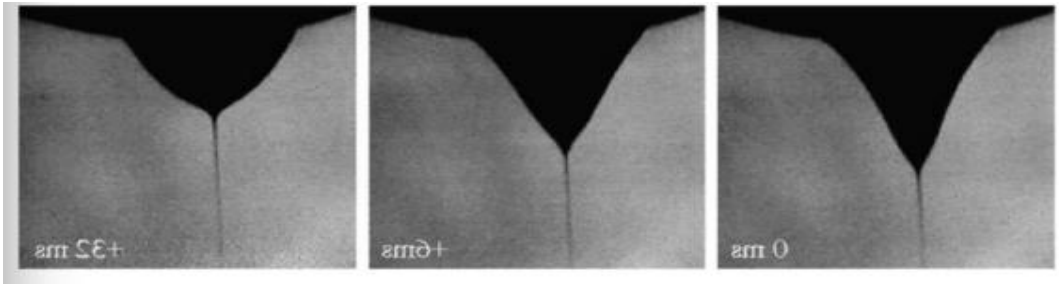

Figure 8:The illustration of the fiber emanated from the droplet

Once the critical voltage is reached, the equilibrium between surface tension and the electric field was becomes equally distributed, leading to the fibers emanated from the tip of Taylor cone as shown in figure 8. The first image of figure 7 showed the elongated and thinning jet flowed from the droplet after the equilibrium was disturbed. This jet was stale and persisted as long as the solution carried away by the jet is replaced by fluid flowing into the droplet.

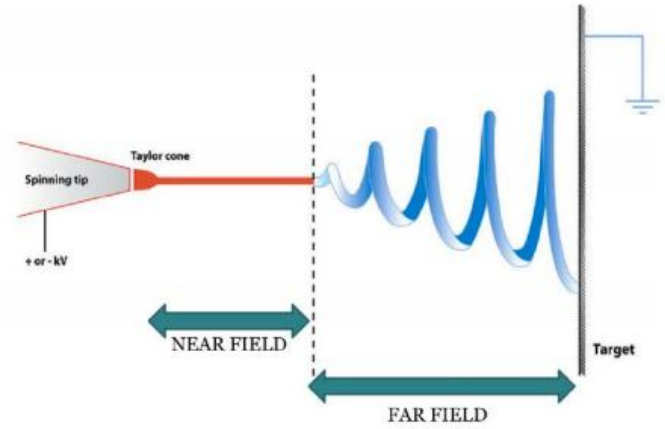

Figure 9: Illustration of the path of the fiber jet during electrospinning process

After the fiber jet is formed and stabilized, it moves straight to the collector but at a certain distance, starts whipping fashion until collected. Figure 9 demonstrates the path of the fiber jet during the electrospinning process. The first regime commonly referred to as near field, provides a stable fiber jet but transitions rapidly at a certain distance into an unpredictable whipping path (far-field electrospinning). The distance of each field heavily determines by the electrospinning parameters. And the diameter of the fiber jet was undergoing a diminishment due to the evaporation of the solvents in the polymer solution and meanwhile the stretching deformation of the fiber jet induced by the electrical field. The whole process was attributed to three instabilities. Basically, the initial straight path was controlled by Rayleigh instability, and the whipping path was explained by bending and whipping instabilities[20], [21]. Theoretically, the Rayleigh instability occurred and became dominated once either the viscosity of the polymer solution is relatively lower or the electric field is smaller[8]. On the contrary, while the electric field is strong enough, the jet would be controlled by bending and whipping instability. During all those processes, a larger amount

of solvent would be evaporated and results in the deposition of ultra-fine fibers on the conductive collector.

1.2.3. Major parameters that influence the deposited fibers

The size, morphology and characteristics of electronspun fibers are influence by many factors, which could be classified into three categories: 1) the solution parameters, 2) the process parameters, and 3) ambient parameters. By tuning these parameters, nanofibers with desired size, properties, and morphologies can be obtained[7].

1.2.3.1. Solution parameters

Polymer solution concentration

The spinnability of the polymers/solvent solution is heavily dependent on the polymer concentration. Low polymer concentrations generate beads or discontinuous fibers. Whereas high polymer concentrations lead to the inability to maintain necessary flow of the solution[7][22]. Most of the polymer solutions follow the power law relationship between solution concentration and fiber diameter which indicates that fiber diameter increases with increasing polymer concentration.

The Molecular weight of the polymer

The Molecular weight of polymer also plays an essential role during the electrospinning process. This influences the viscosity of the solution, which significantly affects the diameter of electrospun fiber. The molecular indicates the extent of polymer chainentanglement in solution. Sufficient degree polymer chains entanglement is a prerequisite ensuring required

viscosity in order to generate fibers[23]. Solution utilizing relatively low molecular weight polymer are prone to producing the beaded-fibers instead of continuous fibers. However, with the increasing molecular weight, the number of beads diminished until the continuous fiber emerged[24]. As a result, the molecular weight of polymer should be directly proportional to the diameter of obtained fibers.

The Viscosity of the polymer solution

The solution viscosity is another crucial factor for electrospinning. For instance, a polymer solution with an extremely low viscosity cannot to produce continuous fibers. On the contrary, its hard for a high-viscous solution to emanate the jet from the droplet due to the high surface tension. As a result, the determination of the optimal viscosity is critical for obtaining the desired fibers.

1.2.3.2. Process parameters

Applied external voltage

The external voltage is a critical factor during the electrospinning process because it provides the necessary force to pull the fiber jet out from the pendant droplet. However, as mentioned before, there is a threshold voltage to initiate the jet, and this critical voltage is determined by many factors, such as surface tension, viscosity, and flow rate. In principle, the electric field is believed to affect the electrospun fibers, but the relationship between them has been debated for many years. For instance, some research suggest that higher voltages generates larger fiber diameter[25]. However, other studies reported that higher voltages produce smaller fibers. They believe the growing voltage increased the repulsive force between each charge located on the surface of the droplet, which results in the

shrinkage of the fibers[26], [27]. Regardless the applied voltage significant influences fiber size, but this trend is also dependent on other factors, such as solution concentration or the working distance between the droplet and collector which will be discussed in following parts.

Flow rate

The flow rate of the polymer solution filled in the syringe influence the size of the electrospun fibers by adjusting the evaporation time of the fibers. Slow flow rates provide sufficient time for the solvent to evaporate in the air. Additionally, the fibers with the smaller diameter are supposed to be obtained. Some researchers observed fibers beading due to the insufficient evaporation or drying time caused by the rapid flow rates[28]–[30].

Working distance

The distance between the tip of droplet and surface of the collector is referred to as the working distance. Just like the flow rate, the working distance influences the size of the obtained fibers by adjusting the solvent drying time or the evaporation time. An appropriate working distance would provide enough drying time to the fibers before it reaches the collector. For example, the small working distances typically result in over-sized fibers or beads which lacks sufficient solvent evaporation time. Other properties influenced by the working distance is the flatness of the deposited fibers, it has been found that the flatter fibers would be electrospun while the working distance is relative closer, however, with a longer working distance, the rounder fibers were observed [31].

Types of collectors

The collectors are the conductive substrates where the fibers are deposited [7]. The extent of the alignment of electrospun fibers was the most influenced factor impacted by the type

of collector. For example, flat conductive collectors would give random and disordered fibers while rotating collectors would lead the aligned deposited fibers.

1.2.3.3. Ambient parameters

Besides the solution and process parameters, ambient parameters, such as humidity and temperature could influence the obtained fibers. For example, some researchers discovered that the relatively higher temperature would yield the smaller fibers by enhancing the evaporation rate[32]. Similarly, a low humidity was also believed to be able to increase evaporation rate[33]. However, the appropriate humidity and temperature should be determined, because the over-rapid evaporation rate sometimes could solidify the droplet at the tip of need and therefore slow down or even inhibit the initiation of the fiber jet.

1.2.4. Types of electrospinning

Based on the working distances between the collector and initiated point of the jet, the electrospinning techniques could be classified into two class: 1) far-field electrospinning and 2) near-field electrospinning. Previously illustrated in Figure 9 , if the collector was placed among the straight motion region, the electrospinning was referred as near-field, whereas if the fibers were deposited within the whipping motion region, the electrospinning was called far-field electrospinning.

Far-field electrospinning

The far-field electrospinning is the most conventional setup, the working distance between the droplet and the collector is approximately 10 cm. Figure 10 is the schematic of the conventional far-field electrospinning with vertical feeding direction, but a horizontal

feeding direction is also common. Figure 11 shows the horizontal feeding direction electrospinning setup. One of the main disadvantages of the conventional far-field electrospinning is the poor alignment of the deposited fibers due to the uncontrollable whipping motion region. Figure 12 was the image of the 11% PAN nanofibers obtained by the in-house far-field electrospinning. According to Figure 12, the electrospun nanofibers are randomly and disorientated on the alumina foil. In addition to the working distance difference, in order to reach the relatively long distance than near-field, the applied voltage of the far-field electrospinning is much larger than the near-field electrospinning. For example, the voltage supply of the in-house far-field setup can provide 20kV while the in-house near- field setup can only provide 1500V.

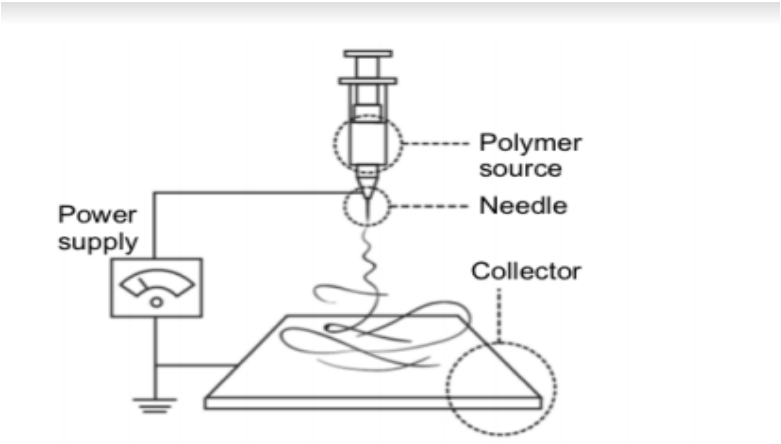

Figure 10: Schematic of a conventional vertical feeding electrospinning setup

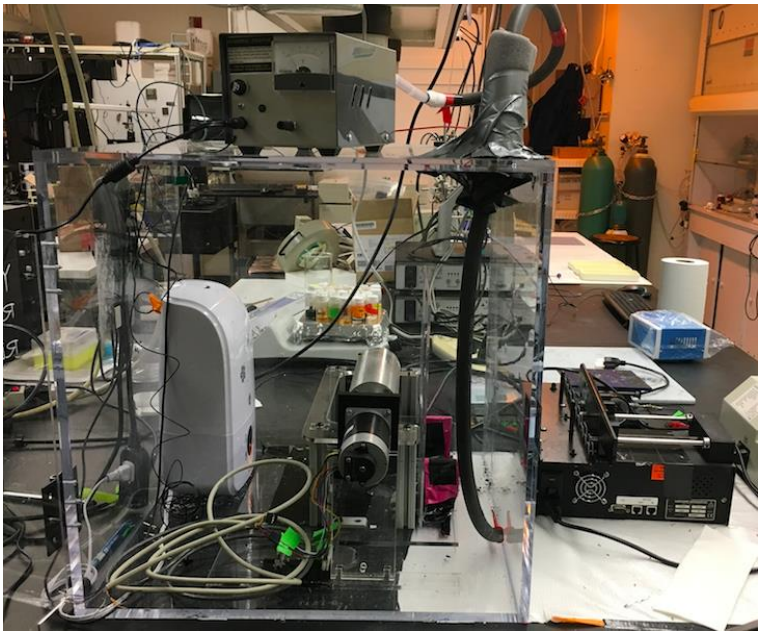

Figure 11: The image of in-house far-field electrospinning setup

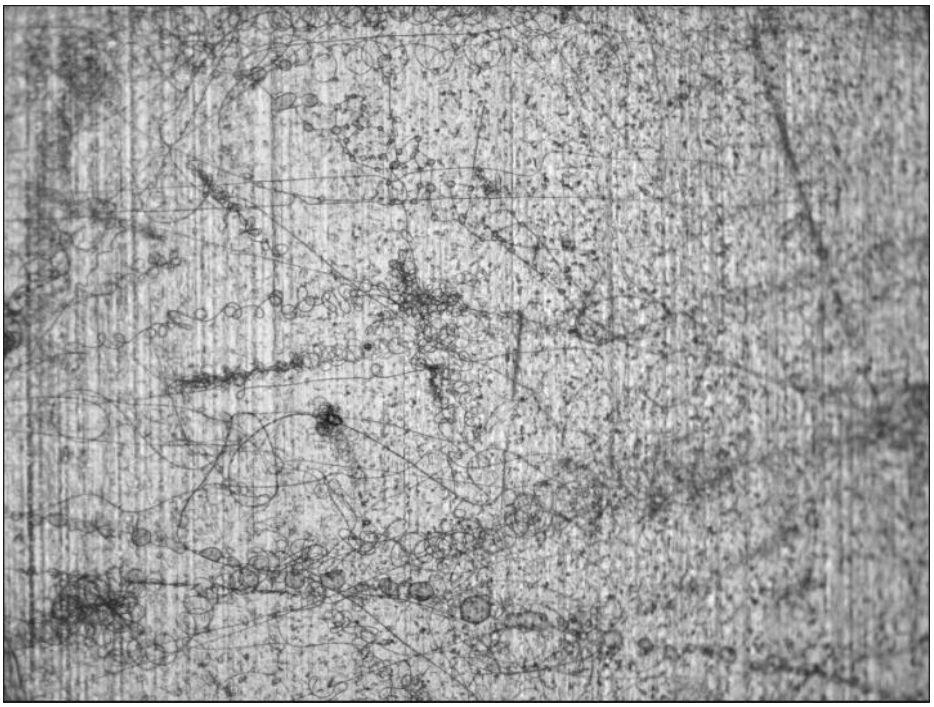

Figure 12: The image of the deposited 10% PAN obtained by the in-house far-field electrospinning

1.42. Near-field electrospinning

Many applications require ordered and aligned nanofibers, such as photonic and electronic devices, unachievable through far-field electrospinning. So, there we introduce the near-field electrospinning, which could provide more predictable and precise control of nanofiber deposition[34]. The main feature of the near-field electrospinning is the short working distance[35]. The most conventional near-field electrospinning setup is called the Electromechanical Spinning(EMS). Figure 13 is the image of the in-house EMS setup.

In principle, it uses a glass rod carrying the opposite charge to initiate the fiber jet from the pendant droplet as figure 14 exhibited. However, even though this setup achieved the precisely controllable deposition, the scalability of this system is still a primary concern that needs to be resolved.

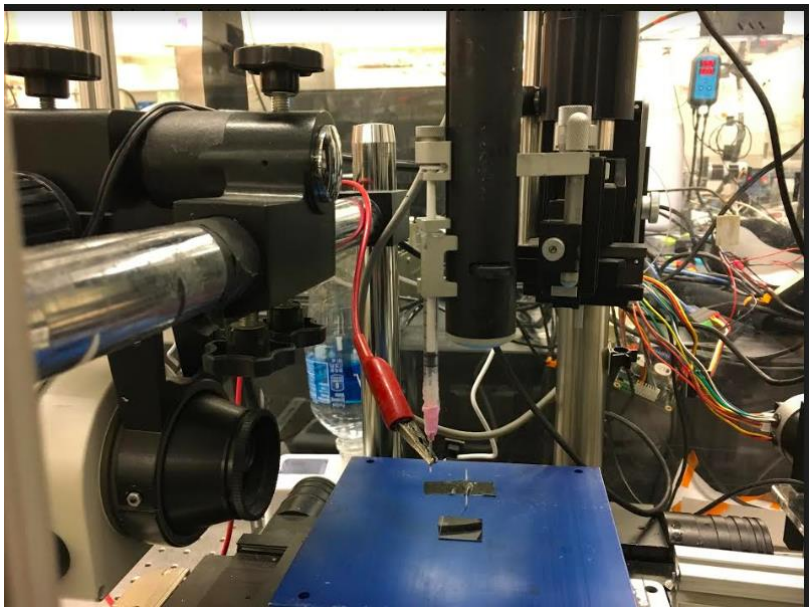

Figure 13: Image of the in-house electromechanical spinning

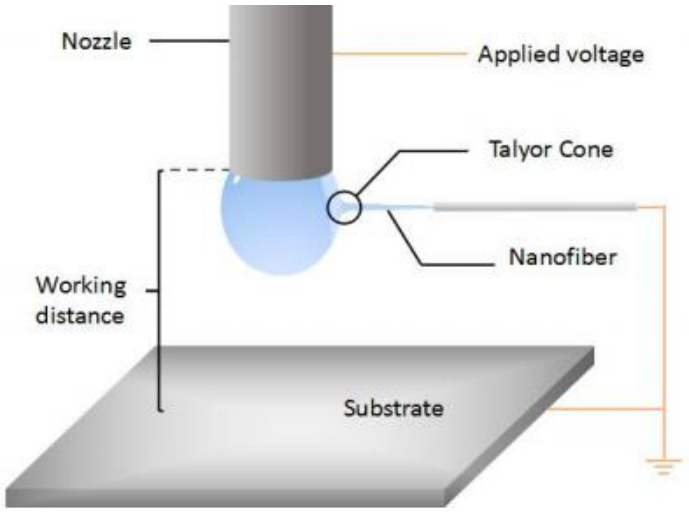

Figure 14: The schematic of EMS process

1.3. The photolithography

The photolithography is the techniques which could transfer 3- dimension geometric structure to a substrate through patterning the photoresist with the UV light shining through a mask with designed pattern on it. The most common substrates are Silicon, Silicon Dioxide, Silicon Nitride, Quartz, and more recently Sapphire. After coating the substrate with the photoresist, this one is then exposed to UV light using a mask to transfer the pattern and developed to form dimensional relief images on the substrates. In general, the ideal photoresist image has the exact shape of the designed pattern in the plane of the substrate, with vertical walls throughout the thickness of the resist. The final resist pattern is binary: parts of the substrate are covered with resist while other parts are completely uncovered. For some applications, the patterned photoresist is the desired structure to fabricate. For other, the binary pattern is needed for transfer using the photoresist as a sacrificial layer,

since the parts of the substrate covered with photoresist will be protected from etching, ion implantation, or other pattern transfer mechanism. The main steps involved in MEMS photolithography process are wafer cleaning and surface preparation, photoresist application, soft baking, mask alignment, UV light exposure, post exposure bake (only negative photoresist), development and hard-baking. There are two types of photoresists: positive and negative. In the case of positive resists, UV light decomposes the resist material, and changes its chemical structure becoming soluble in the developer, and can be removed. Negative resists, on the other hand, behave in just the opposite manner, the area exposed to the UV light get crosslinked and hardened, which is less soluble or completely insoluble in the developer solution. Those steps are summarized in Figure 15, the final step for C-MEMS fabrication would be the pyrolysis.

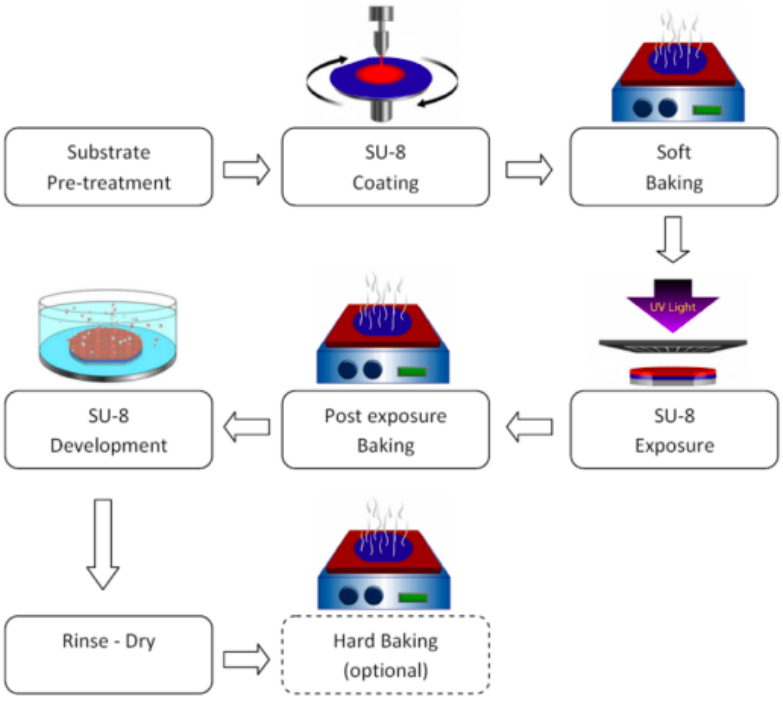

Figure 15: Steps of photolithography process

1.4. pyrolysis

The pyrolysis process to carbonizes the precursor polymer into simple carbon chains. This involves heating up the polymer structure under inert condition. Depending on the temperature receipt, the obtained carbon maybe has various properties, such as porosity, conductivity, and hardness. In this thesis, the photolithography and pyrolysis carried out to fabricate the microstructure to support the suspended fibers.

2.Material and Method

2.1. Polymeric solutions preparation

Polyacrylonitrile (PAN) was a qualified candidate for electrospinning due to its excellent viscosity and conductivity, and this two properties could be manipulated by adding solvent and salt[36][37][38]. In this case, Dimethylformamide (DMF) was the solvent. Figure 16 is the PAN and DMF used in this thesis.

Figure 16: Picture of PAN and its solvent DMF

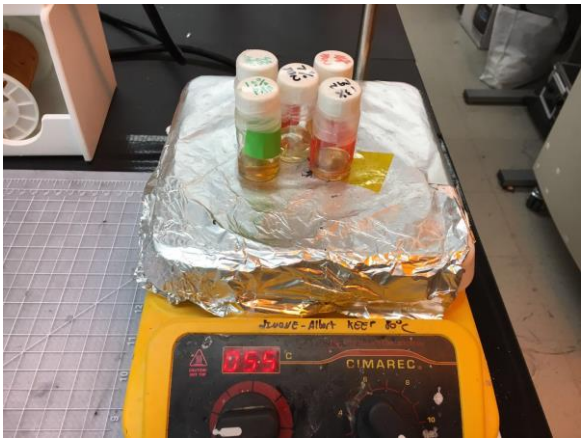

Figure 17: The PAN-based solutions

After mixing PAN and DMF, the PAN-based solution was heated up to 50-60^{o} C to achieve a homogenous solution as Figure 17 showed. The last step of preparation is removing the solution to a syringe. Figure 18 is the syringe filled with 9% of the PAN-based solution, the purpose of wrapping the needle up with the alumina foil is to create a conductive area which would be clamped up the cable of the voltage supply.

Figure 18: The syringe filled with 9% of PAN

2.3. Near-field electrospinning setup

In order to improve the extent of the alignment of deposited nanofibers and scalability, we designed and built a new near-field electrospinning setup. Figure 19 is the picture of the setup we made. Figure 20 is the close-look of the crucial part of the setup. The critical components of this setup include the optical microscopy which could observe pendant droplet the process of the jet initiation, the syringe pump (pointed by an orange arrow in Figure 20) and its controller (Figure 21), a rotating drum (pointed by a blue arrow in Figure 20) whose rotational speed ranged from 500-4000 RPM, moving stage (pointed by a green arrow in Figure 20) and its controller (Figure 22) and a voltage supply which could provide a range of voltage from 0 to 1500V. There is a small piece of silicon wafer (pointed by a red arrow in figure 20) stabilized on the surface of the drum and acted as collector of electrospun fibers. The red cable clamping the needle were connected to the voltage supply. Besides those necessary components, this new setup could also adjust the ambient parameters including the temperature and humidity. For example, the heater (pointed by the blue arrow in Figure 19) located at the left corner could increase the inside temperature of the chamber and the humidifier (pointed by red arrow in figure 19) placed right corner could change the humidity of the chamber.

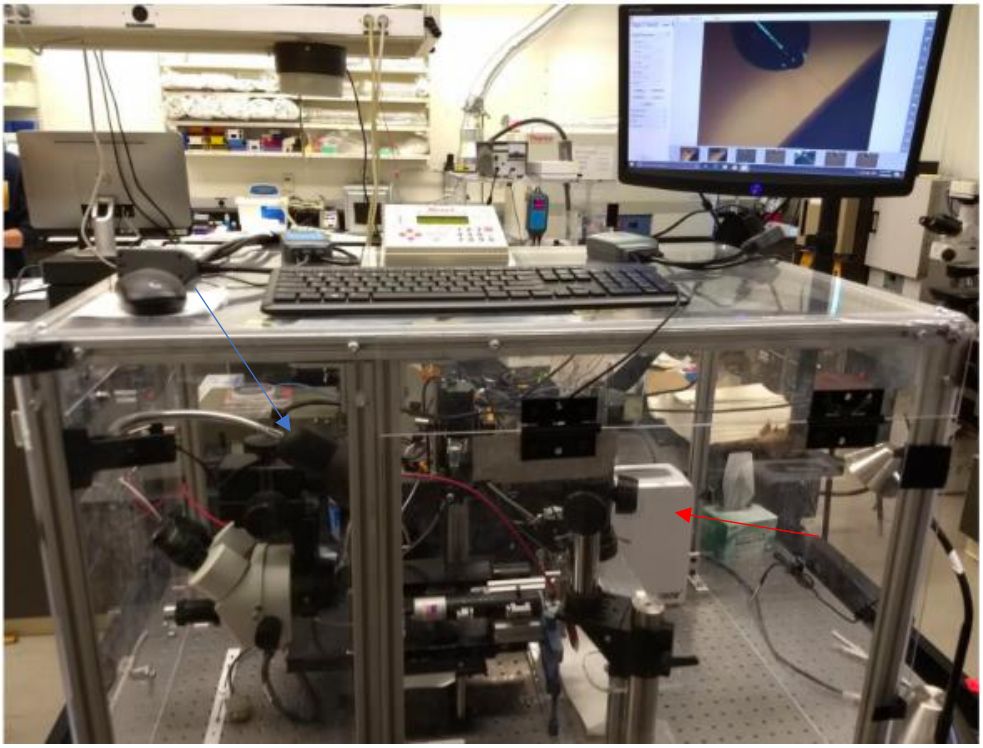

Figure 19: The in-house novel near-field electrospinning setup

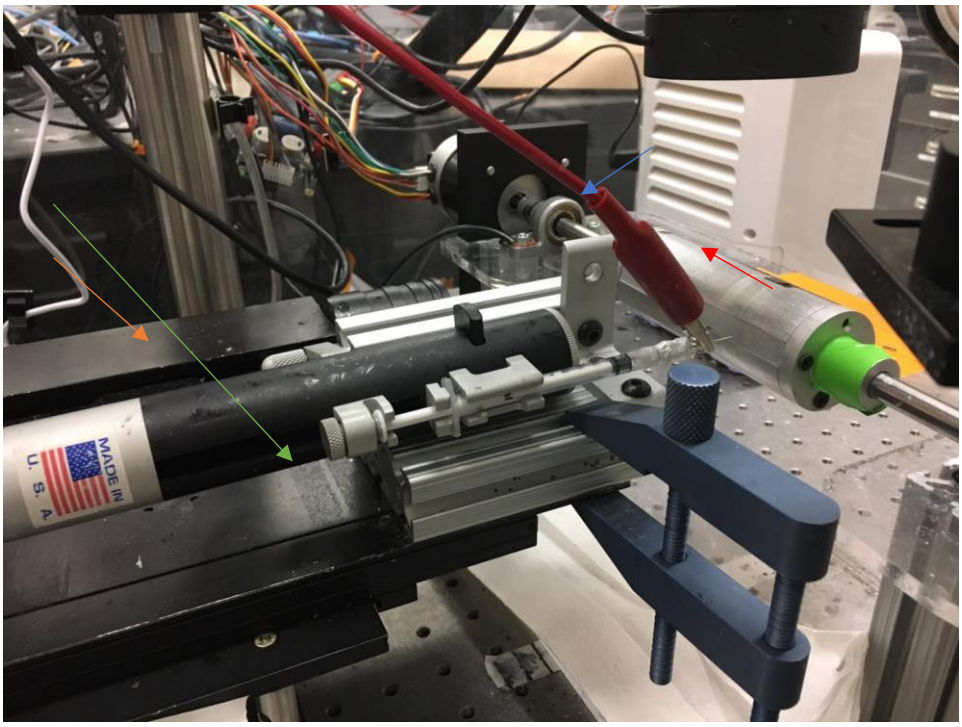

Figure 20: The zoomed-in picture of the crucial syringe setting

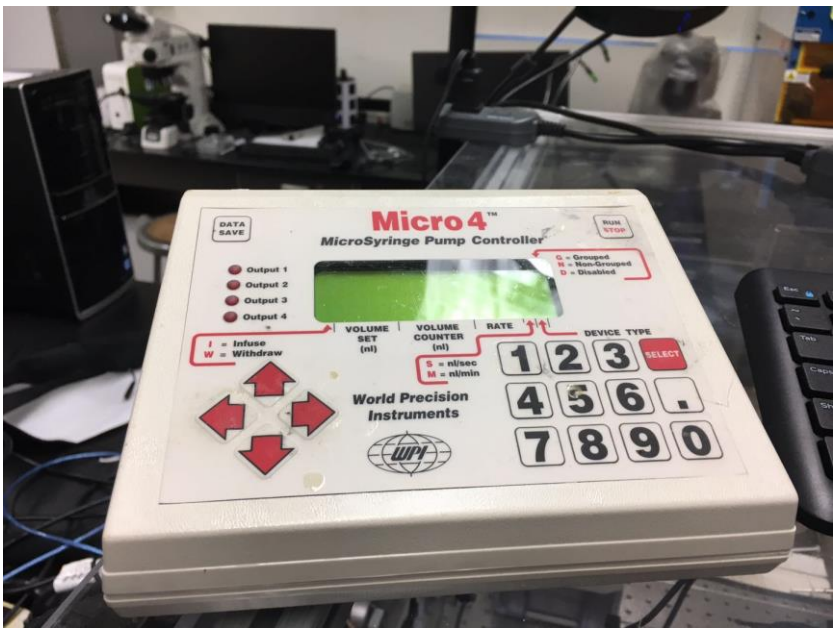

Figure 21: Picture of syringe pump controller

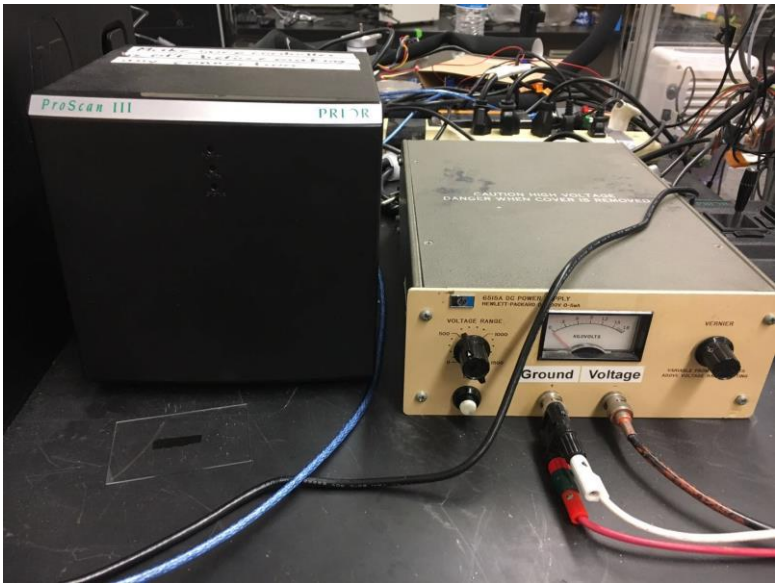

Figure 22: Moving stage controller (right) and voltage supply (left)

2.4 Optimization of the process parameters

According to Figure 20, the syringe filled with PAN solution was stabilized on the pump, the needle was clamped with the red cable which connected to the voltage supply. To figure out the effect of each parameters on the diameter of each fiber and spacing between them, the selected parameter was changed while other parameters were fixated. After each trial, the piece of the silicon wafer was removed from the drum and then examined under the in-house optical microscopy. In this case, the tested parameters are the voltage, stage speed, rotation speed of the drum (RPM), working distance between the drum and needle. The software used to measure the diameter of the fibers and the spacing between each fiber is Image J.

2.5. Fabrication of the supporting structure to nanofibers by photolithography

The nanostructures made by photolithography was used to support the nanofibers and therefore determine the young's modulus of those fibers before and after pyrolysis. The pattern of the supporting structure we made is quite simple, it consists of two thick paralleled walls separated by a gap as figure 23 exhibited. In this case, to test the suspending strength of the fibers, we designed gaps 15um width.

Figure 23: Schematic of supporting structure

2.5.1. Silicon wafer preparation

The silicon wafers were cleaned by deionized water (DI water), acetone and isopropanol (IPA) in order. Then blow dry it with nitrogen gas. The next step is putting the dried wafer into the oven at 120^{o} C for two hours for the further drying.

2.5.2. Photoresist coating

The SU-8 2015 was chosen as the photoresist to fabricate the supporting structure. The thickness of the obtained structure was determined by spinning speed of the spin coater. In this case, the target thickness was 15 μm before pyrolysis. Regarding to this requirement, the spin coater was programmed to reach 500 RPM in 5 second and keep 500 RPM for 10 second, then the spinning speed was accelerated to 4000 RPM in 6 second and stay there for 30 second. Figure 23 illustrate the spin coating of SU-8 2015, in order to obtain the homogenous distribution over the entire surface of wafer and avoid bubbles, the SU-8 should be poured on the center of the wafer.

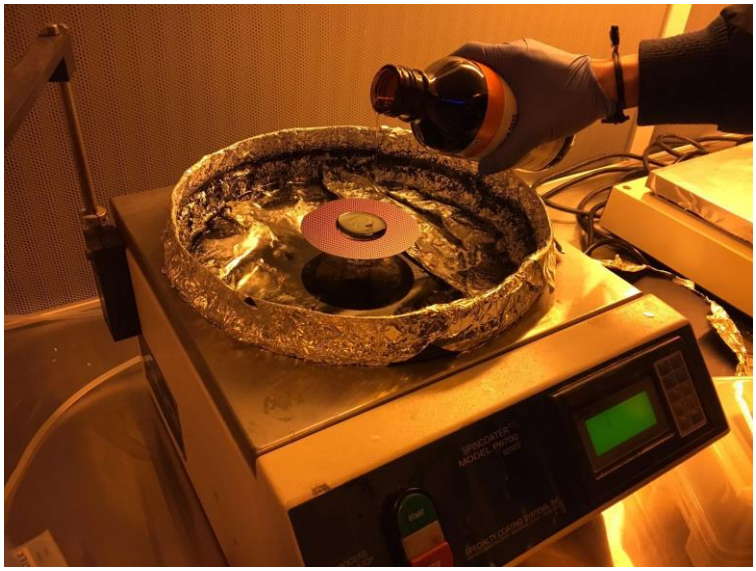

Figure 24: The spin coating for SU-8 2015

2.5.3. Soft-bake

After the photoresist was coated on the wafer, partial evaporation of the photoresist solvent is necessary in order to enhance the homogeneousness, adhesion between SU-8 and wafer and the etching resistance. In this case, a programmable leveled hotplate was used owing to the uniform thermal radiation it could provide. Figure 24 shows that the soft-baking of the coated wafer. According to the SU-8 Supplier, the optimal temperature receipt is exhibited in Figure 25. It's necessary to use a hotplate instead of oven for soft-bake, because it allow the heat radiated from bottom of the wafer. However, if the oven was carried out in this step, the surface of the SU-8 would be dried first and therefore imped the further evaporation of solvent.

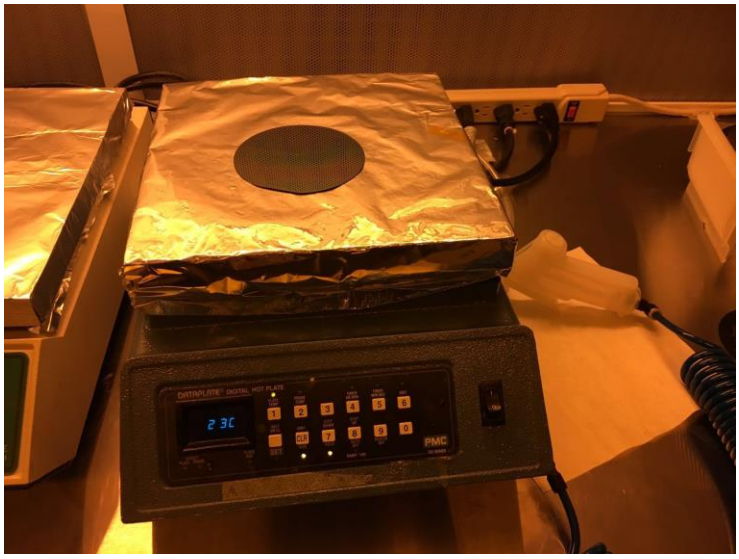

Figure 25: Soft-bake of coated silicon wafer

Figure 26: Temperature Ramp used for soft bake

2.5.4. Expose

The expose step is the critical part of the photolithography, basically, transfers the pattern on the mask to the photoresist coated wafer. The pattern is the design of the supporting structure for the suspended fibers. In this case, we use the UV light to activate the photosensitive component of the exposed part. According to the SU-8 supplier, the optimal exposing time is 140 s.

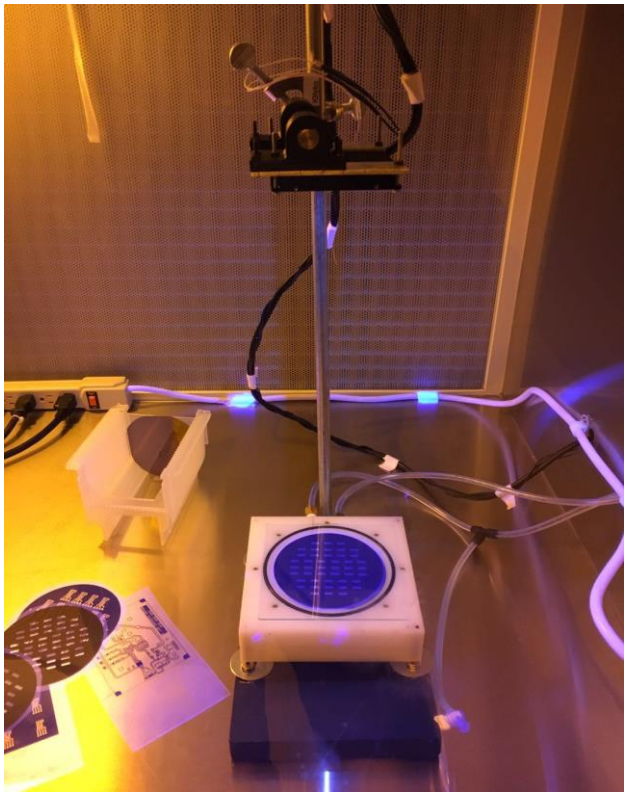

Figure 27: The expose step by using UV radiation

2.5.5. Post-bake

The purpose of post-bake is to remove the residual solvent, according to SU-8 supplier, this step should be carried out at 95^{o} C for 4 minutes regarding to the target thickness(20um).

2.5.6. Development

During this step, the wafer was soaked into the SU-8 developer to removal the part which was not exposed to the UV light. The development time was depended on the thickness. In this case, 4-5 minutes is appropriate. After development, the wafer was washed up by the IPA solution and dried by nitrogen gas.

2.5.7. Hard-bake

The purpose of hard-bake is to further evaporate the residual liquid including SU-8 developer and IPA. In this case, the wafer was placed on the hotplate for half hour at 190^{o}C

2.6. Suspension test of nanofiber

The supporting structure with 15um gap was used as the substrate, the process parameter carried out are 500V of voltage, 1000RPM and 720um/s of stage speed. Since the purpose of this part is to determine the 11% PAN suspension strength, in order to have a better observation, a relative faster stage speed was chosen to deposit less fibers.

3. Results and Conclusions

3.1. Scalability and deposition control

When a fiber is deposited on the rotating drum, it anchors at one point, and rolling process begins. The main problem of the EMS technique is that straight nanowires are hard to obtaine unless the stages speed is rapid enough, for example, if the stage speed wasn't reached the critical value, the curved or coiling nanofiber would be obtained. However, the shear force and fast rotating speed provided by the rotating drum could straighten the nanofibers as Figure 28 showed. Besides the straightening, since the syringe was mounted on a moving stage (Figure 20) could move the syringe along the drum, the alignment of deposited fibers could be achieved. Figure 29 compared the fiber obtained by EMS (left) and new setup with rotating drum (right) at the same voltage and same stage speed, apparently, the rotating drum could give a straighter nanofiber. Another advance of new setup is the high-efficiency or scalability compared to the EMS. Since EMS always use a tiny glass rod to initiate the nanofiber, the whole precise process is harder to control, for example, it takes at less 5-10 minutes to deposited one single fiber for a skillful user. However, it only takes a few minutes to deposit multiple fibers by carrying out the new setup. Figure 30 is the image of deposited multiple nanofibers at a 500 V applied voltage and 480um/s stage speed. It's worthy to mention that the whole deposition process is less than 1 minutes.

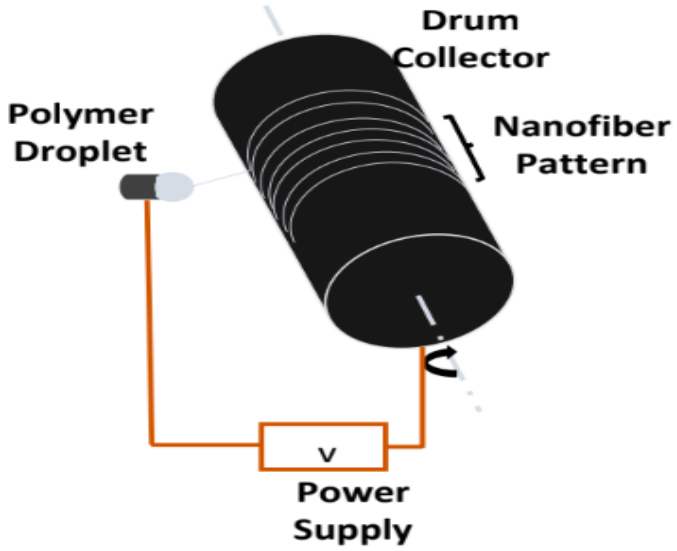

Figure 28: Illustration of the fiber collection by the rotating drum

Figure 29: The nanofiber obtained by EMS (left) and new setup (right) at same applied voltage

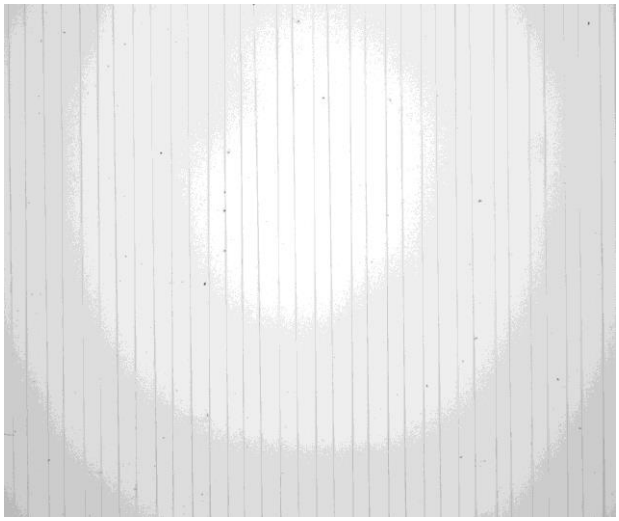

Figure 30: Nanofibers obtained by new setup with 500V, 480um/s stage speed

3.2. Effects of the process parameter on the size of obtained nanofibers

For some applications, such as fabrication of electrodes of super-capacitor and bio-scaffold, the size of the obtained fibers is critical. So, the determination of the relationship between all process parameters and the size of fiber is necessary. After all experiments, we believe the parameters could influence the diameter of obtained fibers are: 1) external applied voltage 2) working distance between the needle and drum 3) rotational speed of the drum.

3.2.1. Voltage versus diameter of fibers

After data analysis, we believe that the diameter of obtained fibers increased with the growing external applied voltages. Figure 31 is the fibers obtained at different voltages, other constant parameters are 1500um in working distance, 720um/s of stage speed, 1500RPM. Obviously, bigger fibers obtained at higher voltages. And Figure 32 show the

trend of diameter with increasing voltage, according it, the maximum diameter is 2.31 um while the applied voltage is 900 V and the minimum diameter is 0.56 um when 400 V voltage was applied. We think reason is that a higher voltage would pull more amount of substance from the solution.

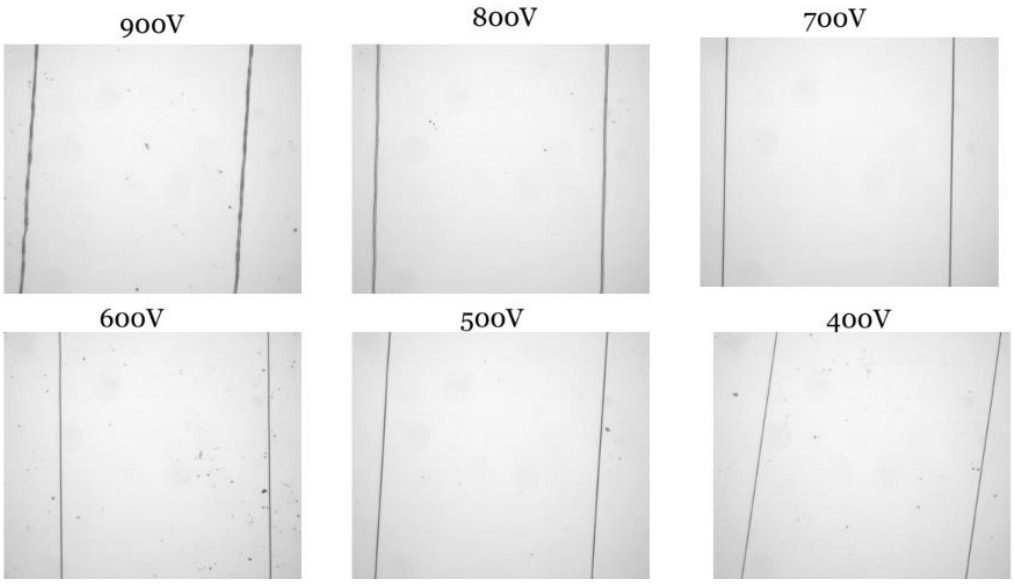

Figure 31: The images of fibers obtained 11% of PAN fibers at different voltages

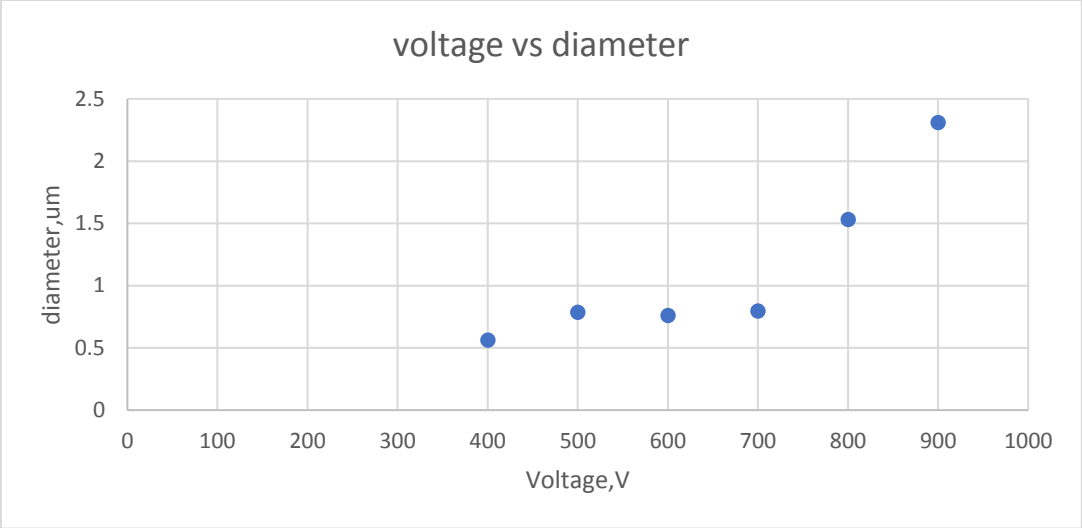

Figure 32: The relationship between Voltage and diameter of fibers

3.2.2.RPM versus diameter of fibers

Figure 33 shows the diameter of obtained fibers at different RPM and Figure 34 exhibit the trend of diameter changes with growing RPM. According to them, the diameter didn't have an obvious change with RPM, we used to expect the higher RPM could decrease the diameter of the fibers because we believe a higher RPM could apply a larger shear force which could render the diameter shrank. However, it turns out the shear force applied by RPM doesn't have much effects on the size of obtained fibers.

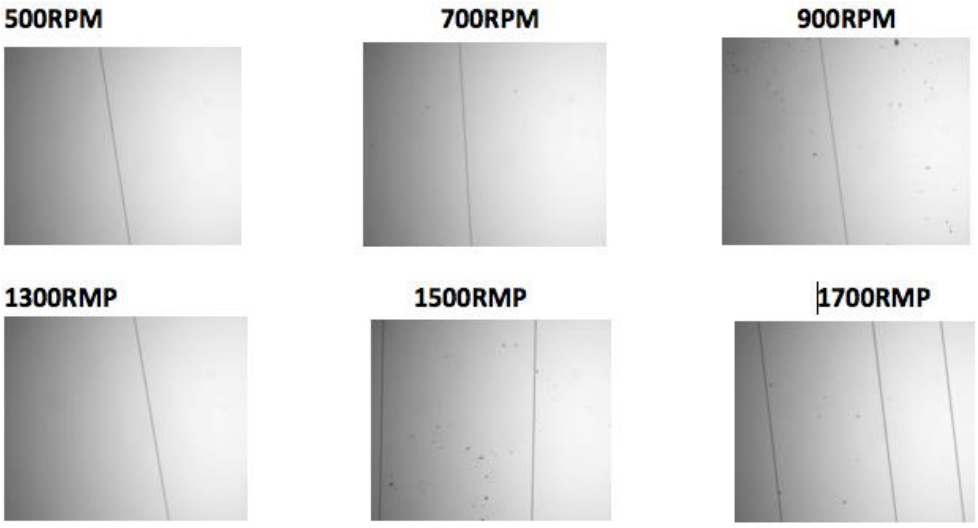

Figure 33: Images of 11% PAN fiber at different RMP

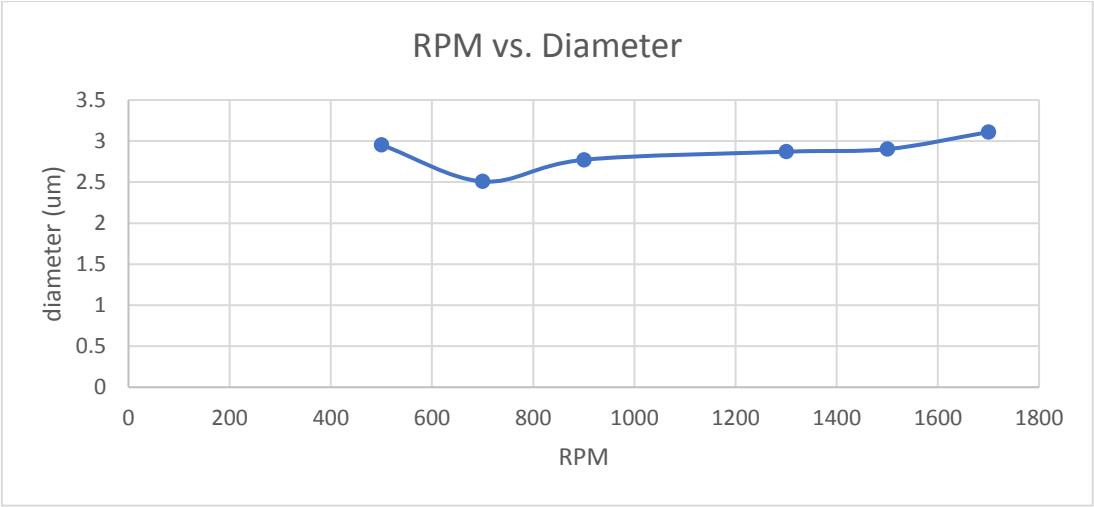

Figure 34: The relationship between diameter of fiber and RPM

3.2.3. Working distance versus diameter

The working distance is the distance between the tip of the needle and the surface of the drum. The diameters of the obtained 11% PAN fibers were measured regarding to various working distance, since other parameter were fixated during the whole process (500V, 500RPM, 120um/s stage speed), the working distance was the only factor influence the size

of the fibers. According the Figure 35, the needle was pulling away from the drum, and the values were measured. Figure 36 is the optical images of obtained fibers regarding to each working distance. The diameter was measured as Table 1 showed, figure 37 exhibit the relationship between the working distance and diameter of fibers. According to results, a longer distance make the fiber shrank. We believe a longer distance give the depositing fiber more time to evaporate the solvent resulting their size shrank.

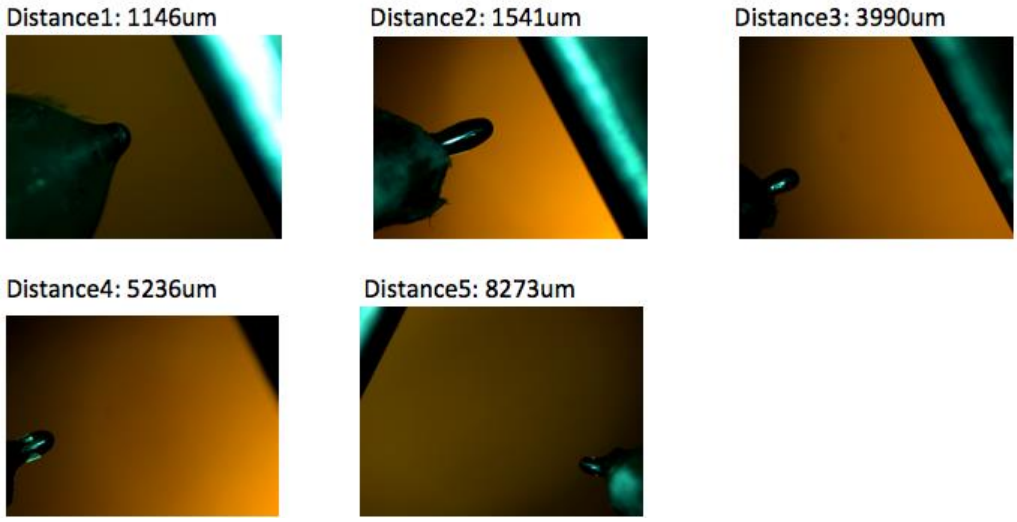

Figure 35: The images of working distances

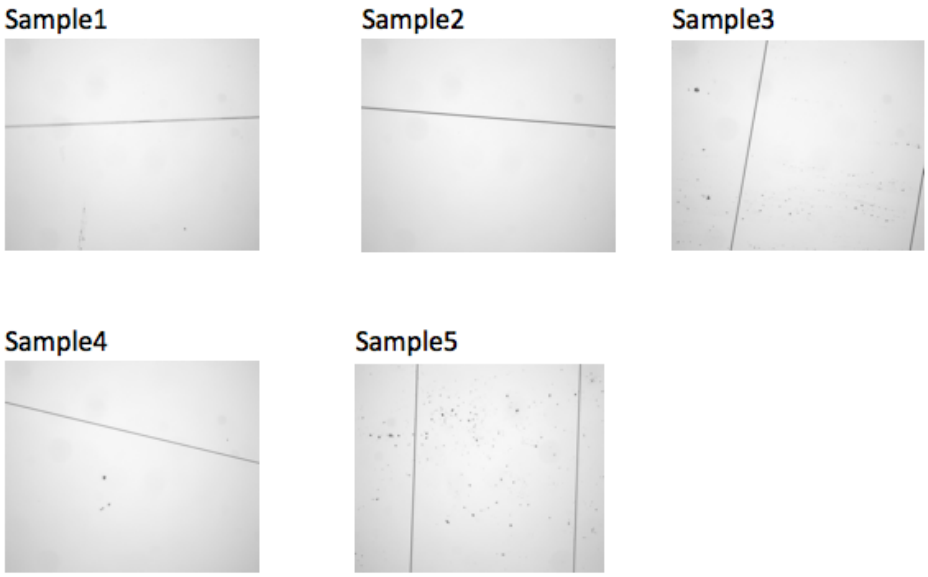

Figure 36: The images of obtained fibers regarding to each distance

Table 1: The working distance and diameter of the fibers

Sample	Working Distance (um)	Diameter of fiber (um)
1	1146	1.9
2	1541	0.498
3	3990	0.487
4	5237	0.319
5	8273	0.284

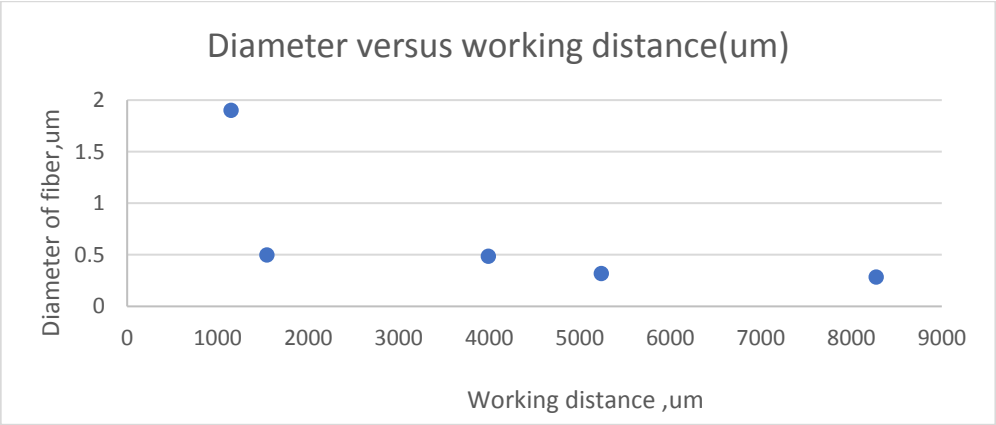

Figure 37: The relationship between working distance and diameter of fibers

3.3. Effects of the process parameter on the spacing between each obtained nanofibers

For some application which needs a significant amount of fibers, such as super-capacitor and filtration, the less spacing between each fiber are required because a less spacing would save spacing for more fibers. We found the stage speed and RPM are the crucial process parameter which influences the spacing most.

3.3.1. The RPM versus spacing

Logically, faster the drum rotated, the less spacing between fibers would be obtained, our results perfectly corroborated this theory. Figure 38 includes some selected images at various RPM, like previous experiments, other parameters are constants (500V, 240um stage speed, 1500 um working distance). According to those images, it's obvious to conclude that a higher RPM would bring down the spacing between each fiber. Table 2 provided more data, and Figure 40 showed the relationship between RPM and spacing.

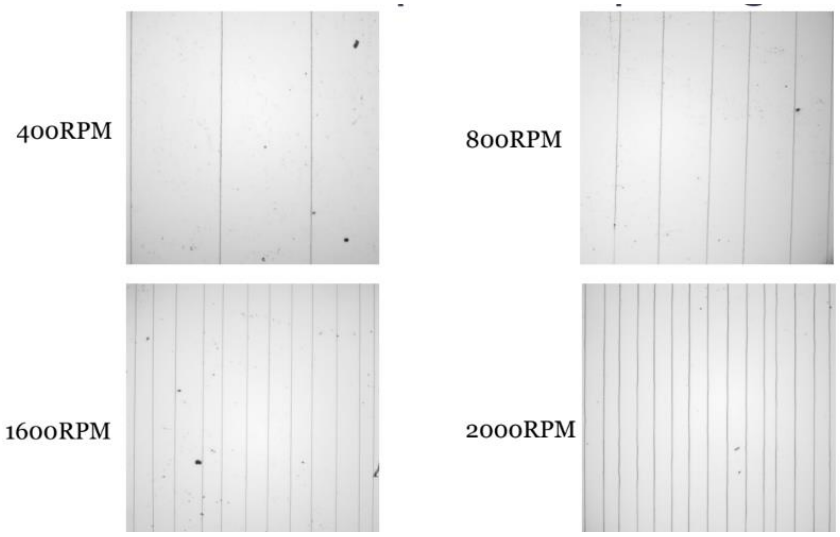

Figure 38: Some selected images of 11% of PAN fibers obtained at various RPM

Table 2:The value of RPM and spacing between fibers

RPM	Spacing(um)
500	384.4715
1000	178.905
2000	90.155
2500	74.86
3000	57.75

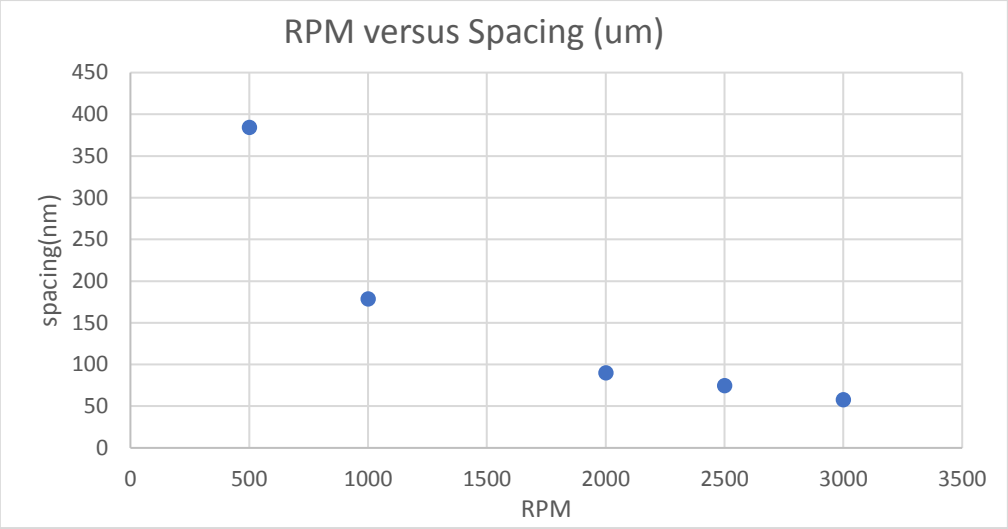

Figure 39: Relationship between RPM and spacing

3.3.2. Stage speed versus RPM

Stage speed should be the most obvious factor that influences the spacing between each fiber. Logically, a slower stage speed would bring down the spacing between fibers, and our results substantiated this assumption. In this case, other constant parameters are 500V, 500RPM, 1500um of working distance. Some selected images of deposited fibers proved that stage speed has a profound impact on spacing. Table 3 gives more information, and Figure 41 shows the relationship between stage speed and spacing.

Figure 40: Some selected images of fibers obtained at various stage speed

Table 3: The stage speed and the resulting spacing between fibers

stage speed (um/s)	Spacing (um)
1680	515.3
1440	445.65
1200	370.04
960	291.72
720	222.99
480	179.68
240	70.66
60	18.25

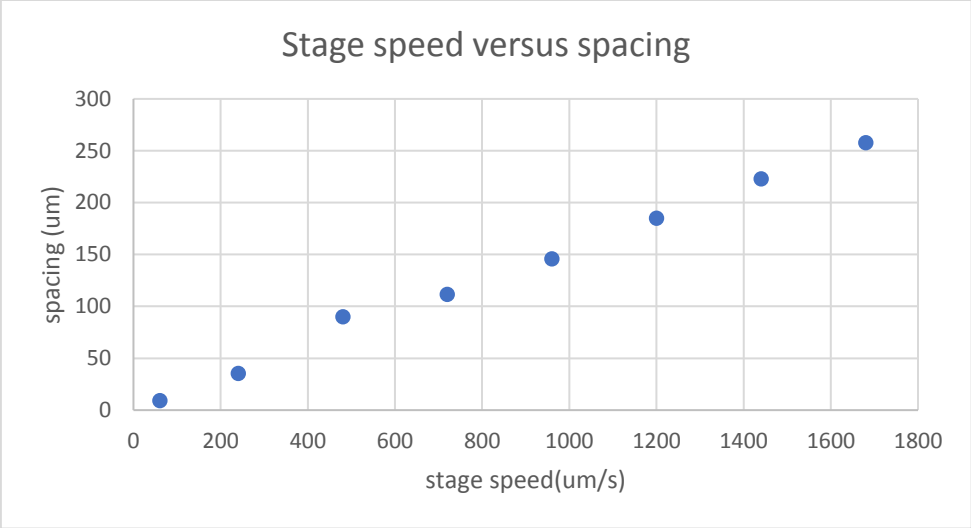

Figure 41: The relationship between stage speed and inter-fiber spacing

3.4. Suspension test of fiber

Figure 42 was the optical image of suspended fiber on a supporting structure with a 15um width. According to whether the fibers out of the photo, the suspended or dripped fibers could be determined. So, we can see those fibers are partially suspended, the green arrow pointed to those fibers which touched the ground, and the red arrow pointed the suspended fibers, the suspended or dripped fibers could be determined. As a result, we could draw a conclusion that the 11% PAN maybe not suitable to produce suspended fibers.

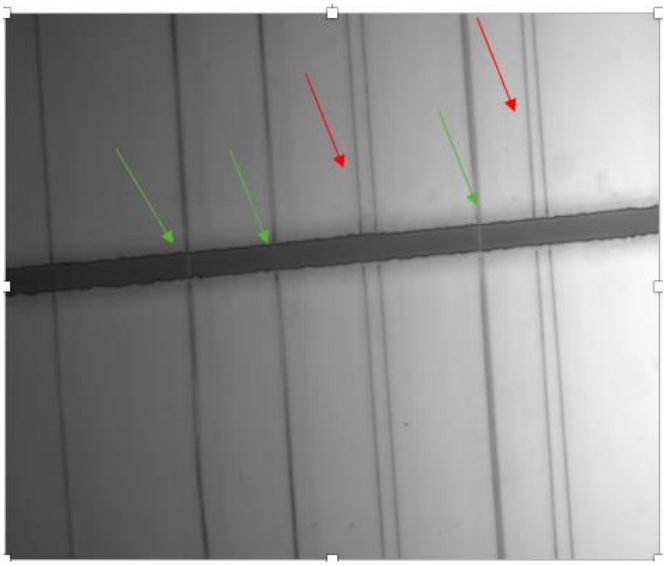

Figure 42: The suspended or dripped fibers made by 11% PAN

4.Furture works

For some application, suspension strength of the fiber is very significant, for example, the gas sensor and electrodes of super-capacitor. Because they both require a higher ratio of surface area to volume. However, for this thesis, the investigation on suspension strength are lacked, first, the optical microscopy is difficult to make an absolute decision whether fibers were suspended. Regarding this problem, scanning electron microscopy (SEM) and transmission electron microscopy (TEM) should be applied. On the other hand, suspension strength or young's modulus of the suspended fiber should be determined as well, in this case, the atomic force microscopy (AFM) might need to be used. In addition, to increase the contacting surface area, a woven or multiple layers of nanofibers could be made, in fact, the author is currently working on this and already successfully make a nanofiber woven by 11% of PAN (Figure 43). But due to it's still in the process, more effort need to be contributed to this part.

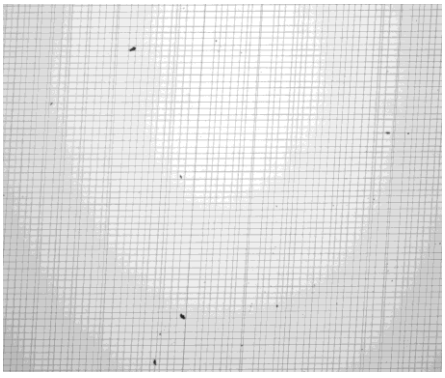

Figure 43: The hole at the back of chamber

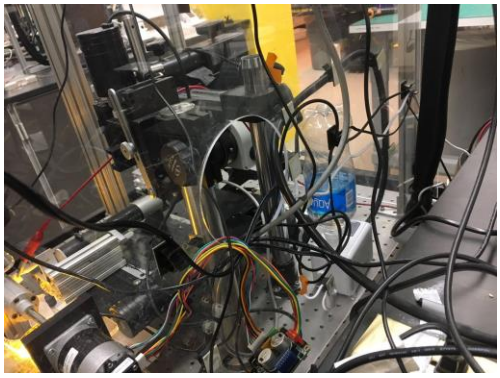

Figure 44: Nanofibers in the form of woven

Since all the result presented are based on the fibers before pyrolysis, in the future, the optimal pyrolysis temperature receipt is needed to be figured out. Otherwise, an

inappropriate temperature receipt could yield discontinuous fibers or incomplete carbonization.

Another part of the future work could be the determination of effects of the ambient parameters. Although the new setup has the heater and humidifier, the author didn't find the relationship between them and the obtained fibers. The author believes this could be attributed to the un-airtight chamber. As we can see from the Figure 44, to get all the cables into the chamber a big hole must be drilled. So, the next step corresponding to this problem should be the building of a more advanced chamber.

Although there are some shortcoming and unfinished work for this project, the obtained results have proved this new setup could salable manufacture aligned nanofibers.

5. Bibliography

[1] *Springer Handbook of Nanotechnology*. 2010.

[2] V. Cimalla, J. Pezoldt, and O. Ambacher, "Group III nitride and SiC based MEMS and NEMS: Materials properties, technology and applications," *J. Phys. D. Appl. Phys.*, vol. 40, no. 20, pp. 6386–6434, 2007.

[3] C. M. Lentz, M. A. Haque, H. C. Foley, and B. A. Samuel, "Synthesis and characterization of glassy carbon nanowires," *J. Nanomater.*, vol. 2011, 2011.

[4] K. Balasubramanian, "Challenges in the use of 1D nanostructures for on-chip biosensing and diagnostics: A review," *Biosensors and Bioelectronics*, vol. 26, no. 4. pp. 1195–1204, 2010.

[5] P. Katta, M. Alessandro, R. D. Ramsier, and G. G. Chase, "Continuous electrospinning of aligned polymer nanofibers onto a wire drum collector," *Nano Lett.*, vol. 4, no. 11, pp. 2215–2218, 2004.

[6] L. Sultan Lipol and M. Moshiur Rahman, "Electrospinning and Electrospun Nanofibers," *World J. Nano Sci. Eng.*, vol. 6, no. June, pp. 45–50, 2016.

[7] N. Bhardwaj and S. C. Kundu, "Electrospinning: A fascinating fiber fabrication technique," *Biotechnol. Adv.*, vol. 28, no. 3, pp. 325–347, 2010.

[8] A. Baji, Y. W. Mai, S. C. Wong, M. Abtahi, and P. Chen, "Electrospinning of polymer nanofibers: Effects on oriented morphology, structures and tensile properties," *Compos. Sci. Technol.*, vol. 70, no. 5, pp. 703–718, 2010.

[9] Y. Sun, F. Wang, W. Zhang, Z. Shao, and C. Ru, "Electrospinning system with tunable

collector for fabricating three-dimensional nanofibrous structures," *Micro & Nano Lett.*, vol. 9, no. 1, pp. 24–27, 2014.

[10] Z. M. Huang, Y. Z. Zhang, M. Kotaki, and S. Ramakrishna, "A review on polymer nanofibers by electrospinning and their applications in nanocomposites," *Compos. Sci. Technol.*, vol. 63, no. 15, pp. 2223–2253, 2003.

[11] B. Vonnegut and R. L. Neubauer, "Production of monodisperse liquid particles by electrical atomization," *J. Colloid Sci.*, vol. 7, no. 6, pp. 616–622, 1952.

[12] P. K. Baumgarten, "Electrostatic spinning of acrylic microfibers," *J. Colloid Interface Sci.*, vol. 36, no. 1, pp. 71–79, 1971.

[13] Q. P. Pham, U. Sharma, and A. G. Mikos, "Electrospinning of Polymeric Nanofibers for Tissue Engineering Applications: A Review," *Tissue Eng.*, vol. 0, no. 0, p. 060509065116001, 2006.

[14] X. Hu, S. Liu, G. Zhou, Y. Huang, Z. Xie, and X. Jing, "Electrospinning of polymeric nanofibers for drug delivery applications," *J. Control. Release*, vol. 185, no. 1, pp. 12–21, 2014.

[15] P. W. Gibson, H. L. Schreuder-Gibson, and D. Rivin, "Electrospun fiber mats: Transport properties," *AIChE J.*, vol. 45, no. 1, pp. 190–195, 1999.

[16] B. Ding, M. Wang, J. Yu, and G. Sun, "Gas sensors based on electrospun nanofibers," *Sensors*, vol. 9, no. 3, pp. 1609–1624, 2009.

[17] R. Jose, P. S. Archana, A. Le Viet, M. V. Reddy, M. M. Yusoff, and S. Ramakrishna, "Electrospun metal oxides nanostructures for energy related devices," *2011 IEEE 1st Conf. Clean Energy Technol. CET 2011*, pp. 161–165, 2011.

[18] G. S. Bisht *et al.*, "Controlled continuous patterning of polymeric nanofibers on three-

dimensional substrates using low-voltage near-field electrospinning," *Nano Lett.*, vol. 11, no. 4, pp. 1831–1837, 2011.

[19] L. A. Mercante, V. P. Scagion, F. L. Migliorini, L. H. C. Mattoso, and D. S. Correa, "Electrospinning-based (bio)sensors for food and agricultural applications: A review," *TrAC - Trends Anal. Chem.*, vol. 91, pp. 91–103, 2017.

[20] D. H. Reneker, A. L. Yarin, H. Fong, and S. Koombhongse, "Bending instability of electrically charged liquid jets of polymer solutions in electrospinning," *J. Appl. Phys.*, vol. 87, no. 9 I, pp. 4531–4547, 2000.

[21] Y. M. Shin, M. M. Hohman, M. P. Brenner, and G. C. Rutledge, "Experimental characterization of electrospinning: the electrically forced jet and instabilities," *Polymer (Guildf).*, vol. 42, no. 25, pp. 09955–09967, 2001.

[22] J. Eyitouyo, "Regeneration of bombyx mori silk nanofibers and nanocomposite fibrils by the electrospinning process," 2005.

[23] M. Mohammadian and A. K. Haghi, "Systematic parameter study for nano-fiber fabrication via electrospinning process," *Bulg. Chem. Commun.*, vol. 46, no. 3, pp. 545–555, 2014.

[24] P. Gupta, C. Elkins, T. Long, and G. Wilkes, "ELECTROSPINNING OF LINEAR HOMOPOLYMERS OF POLY(METHYL METHACRYLATE):EXPLORING RELATIONSHIPS BETWEEN FIBER FORMATION, VISCOSITY, MOLECULAR WEIGHT AND CONCENTRATION IN A GOOD SOLVENT†," 2004, pp. 71–98.

[25] C. Zhang, X. Yuan, L. Wu, Y. Han, and J. Sheng, "Study on morphology of electrospun poly(vinyl alcohol) mats," *Eur. Polym. J.*, vol. 41, no. 3, pp. 423–432, 2005.

[26] L. Larrondo and R. S. J. Manley, "Electrostatic fiber spinning from polymer melts. II.

Examination of the flow field in an electrically driven jet," *... Polym. Sci. Polym. ...*, vol. 19, pp. 921–932, 1981.

[27] L. Larrondo and R. St. John Manley, "Electrostatic fiber spinning from polymer melts. III. Electrostatic deformation of a pendant drop of polymer melt," *J. Polym. Sci. Polym. Phys. Ed.*, vol. 19, no. 6, pp. 933–940, 1981.

[28] L. Wannatong, A. Sirivat, and P. Supaphol, "Effects of solvents on electrospun polymeric fibers: Preliminary study on polystyrene," *Polym. Int.*, vol. 53, no. 11, pp. 1851–1859, 2004.

[29] X. Y. Yuan, Y. Y. Zhang, C. Dong, and J. Sheng, "Morphology of ultrafine polysulfone fibers prepared by electrospinning," *Polym. Int.*, vol. 53, no. 11, pp. 1704–1710, 2004.

[30] W. Zuo, M. Zhu, W. Yang, H. Yu, Y. Chen, and Y. Zhang, "Experimental study on relationship between jet instability and formation of beaded fibers during electrospinning," *Polym. Eng. Sci.*, vol. 45, no. 5, pp. 704–709, 2005.

[31] C. J. Uchko, L. C. Chen, Y. Shen, and D. C. Martina, "Processing and microstructural characterization of porous biocompatible\rprotein polymer thin films," *Polymer (Guildf).*, vol. 40, pp. 7397–7407, 1999.

[32] C. Mit-uppatham, M. Nithitanakul, and P. Supaphol, "Ultratine electrospun polyamide-6 fibers: Effect of solution conditions on morphology and average fiber diameter RID C-4353-2008," *Macromol. Chem. Phys.*, vol. 205, no. 17, pp. 2327–2338, 2004.

[33] C. L. Casper, J. S. Stephens, N. G. Tassi, D. B. Chase, and J. F. Rabolt, "Controlling surface morphology of electrospun polystyrene fibers: Effect of humidity and molecular weight in the electrospinning process," *Macromolecules*, vol. 37, no. 2, pp.

573–578, 2004.

[34] C. Chang, K. Limkrailassiri, and L. Lin, “Continuous near-field electrospinning for large area deposition of orderly nanofiber patterns,” *Appl. Phys. Lett.*, vol. 93, no. 12, pp. 1–4, 2008.

[35] X. X. He *et al.*, “Near-Field Electrospinning: Progress and Applications,” *J. Phys. Chem. C*, vol. 121, no. 16, pp. 8663–8678, 2017.

[36] X. H. Qin, E. L. Yang, N. Li, and S. Y. Wang, “Effect of different salts on electrospinning of polyacrylonitrile (PAN) polymer solution,” *J. Appl. Polym. Sci.*, vol. 103, no. 6, pp. 3865–3870, 2007.

[37] J. H. He, Y. Q. Wan, and J. Y. Yu, “Effect of concentration on electrospun polyacrylonitrile (PAN) nanofibers,” *Fibers Polym.*, vol. 9, no. 2, pp. 140–142, 2008.

[38] S. Y. Gu, J. Ren, and Q. L. Wu, “Preparation and structures of electrospun PAN nanofibers as a precursor of carbon nanofibers,” *Synth. Met.*, vol. 155, no. 1, pp. 157–161, 2005.